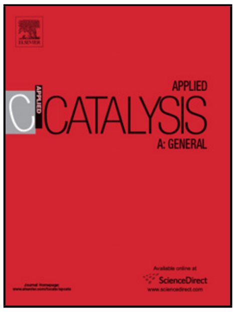

Title: Ionic ammonium and anilinium based polymolybdate hybrid catalysts for olefin epoxidation

Authors: Barbara Bożek, Patrícia Neves, Wiesław Łasocha, Anabela A. Valente

PII: S0926-860X(18)30324-7
DOI: https://doi.org/10.1016/j.apcata.2018.07.001
Reference: APCATA 16727

To appear in: *Applied Catalysis A: General*

Received date: 18-3-2018
Revised date: 17-5-2018
Accepted date: 1-7-2018

Please cite this article as: Bożek B, Neves P, Łasocha W, Valente AA, Ionic ammonium and anilinium based polymolybdate hybrid catalysts for olefin epoxidation, *Applied Catalysis A, General* (2018), https://doi.org/10.1016/j.apcata.2018.07.001

Ionic ammonium and anilinium based polymolybdate hybrid catalysts for olefin epoxidation

Barbara Bożek[a,†], Patrícia Neves[b,†], Wiesław Łasocha[a,c,*], Anabela A.Valente[b,*]

[a]*Jerzy Haber Institute of Catalysis and Surface Chemistry, Polish Academy of Sciences, Niezapominajek 8, 30-239 Krakow, Poland*
[b]*Department of Chemistry, CICECO – Aveiro Institute of Materials, University of Aveiro, 3810-193 Aveiro, Portugal*
[c]*Faculty of Chemistry, Jagiellonian University, ul. Gronostajowa 2, 30-387 Krakow, Poland*

[†]These authors contributed equally to this work.

[*]Corresponding authors. Fax: +351 234 401470.

E-mail addresses: atav@ua.pt (A.A. Valente), nclasoch@cyf-kr.edu.pl (W. Łasocha).

Graphical abstract

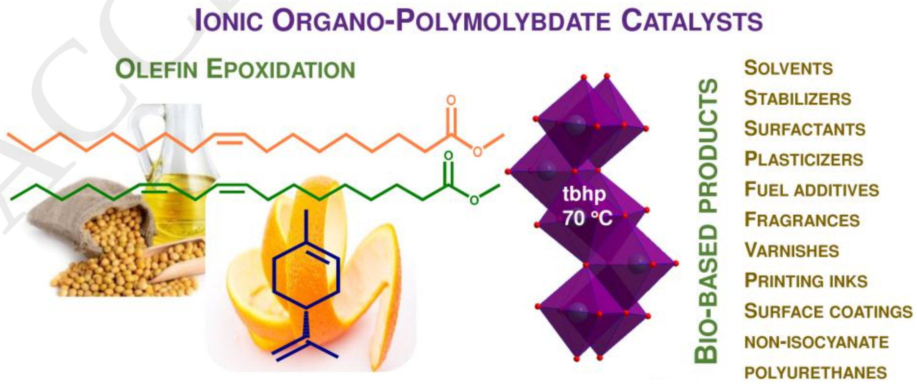

Highlights

- Ionic organo-polymolybdate hybrids (IPHs) easily synthesised under mild, aqueous phase conditions

- Type of synthetic organic precursor and synthesis conditions influence structural features of IPHs, influencing catalytic performance

- The best-performing catalyst possessed one-dimensional structure and selectively converted biomass-derived olefins to the respective epoxides

- The best-performing catalyst possessed steady activity in consecutive batch runs, with preservation of structural features

Abstract

Ionic polymolybdate hybrids (IPH) are interesting catalysts for liquid phase olefin epoxidation with *tert*-butylhydroperoxide (*t*bhp), e.g. conversion of terpenic and fatty acid methyl ester (FAME) components of biomass to useful bio-products. IPHs may be easily prepared, under clean, mild, aqueous phase conditions. The type of organic precursor and the synthesis conditions infleunce the structural features of the IPHs. In this work, IPH epoxidation catalysts possessing one- (1-D) or two-dimensional (2-D) structures were investigated, which included the new materials 1-D methylammonium

ammonium trimolybdate $[CH_3NH_3\cdot NH_4\cdot Mo_3O_{10}]$ (**1**) and 2-D bis(2,5-dimethylanilinium) pentamolybdate $[Mo_5O_{16}\cdot 2(NH_3C_6H_3(CH_3)_2)]$ (**4**) with solved structures, and 1-D bis(3,5-dimethylanilinium) trimolybdate $[Mo_3O_{10}\cdot 2(NH_3C_6H_3(CH_3)_2)]$ (**2**), bis(4-methylanilinium) trimolybdate $[Mo_3O_{10}\cdot 2(NH_3C_6H_4CH_3)]$ (**3**), 2-D bis(anilinium) pentamolybdate $[Mo_5O_{16}\cdot 2(NH_3C_6H_5)]$ (**5**), bis(4-methylanilinium) pentamolybdate $[Mo_5O_{16}\cdot 2(NH_3C_6H_4CH_3)]$ (**6**) and bis(4-ethylanilinium) pentamolybdate $[Mo_5O_{16}\cdot 2(NH_3C_6H_4C_2H_5)]$ (**7**). Systematic characterisation and catalytic studies helped gain insights into structure-activity relationships. The best-performing catalyst (**2**) was effective for the epoxidation of the FAMEs such as, methyl oleate which gave 92 % methyl 9,10-epoxyoctadecanoate yield, at 99 % conversion, at 70 °C. The reaction conditions (temperature, type of cosolvent and oxidant) influenced the catalytic reaction. Catalytic performance in consecutive batch runs was steady, and the structural features were essentially preserved.

Keywords: polymolybdates; hybrids; crystal structure; catalytic epoxidation; bio-derived olefins

1. Introduction

The development of catalysts for chemical processes with reduced carbon footprint, following green chemistry principles, is important. Catalytic epoxidation is a valuable tool to convert unsaturated fatty acid methyl esters (FAMEs) and terpenic components of (renewable) vegetable biomass to bio-products with wide application profiles. Interesting FAMEs include methyl oleate (Ole) and methyl linoleate (LinOle), which are readily available in nature; e.g. canola, soybean, sunflower and corn oils (Scheme 1). Epoxidised FAMEs can act as alternative plasticizers/stabilizers for PVC production, solvents [1], surface coatings [2,3] surfactants [4], biodegradable lubricants [5], fuel additives [6] and as intermediates for producing resins[2] and polyols used for polyurethane foams production [7]. On the other hand, terpenes are natural, abundant, inedible and relatively inexpensive building blocks, useful for different industrial sectors. In particular, limonene (Lim), a terpene which is extracted from citrus oil and pine wood [8], may be converted to interesting bio-products such as, 1,2-epoxy-*p*-menth-8-ene (LimOx), 1,2:8,9-diepoxy-*p*-menthane (LimDiOx) and 1-methyl-4-(1-methylethenyl)-1,2-cyclohexanediol (LimDiOH) (Scheme 1). LimOx may be used as fragrance, solvent, and for producing metal coatings, varnishes, and printing inks [9,10]; the reaction of LimOx with succinic anhydride affords value-added polyesters [11]. LimDiOx is industrially used as a diluent for epoxy resin and as a solvent [12,13]. Mono- or diepoxides of limonene are interesting monomers for producing biodegradable non-isocyanate polyurethanes (an attractive green alternative to traditional isocyanate polyurethanes, avoiding toxic monomers and phosgene), and thermosetting polymers via copolymerization with CO_2 [10,12-15].

Some industrial processes of FAMEs epoxidation involve the use of peracids as oxidising agents, and strong mineral acids as catalysts, which may present several drawbacks including low product selectivity, corrosion of equipment, and considerable waste production [9]. On the other hand, it is desirable to substitute commercial Lim/peracid stoichiometric epoxidation processes for alterative eco-friendly catalytic routes [16]. In this sense, the use of versatile transition metal catalysts and hydroperoxide oxidants may be advantageous.

In particular, polyoxometalates are versatile inorganic compounds, which have made part of innovative research themes related to crystal engineering, molecular magnets, novel surfactants, medicine, catalysis, etc. [17-31]. In general, polyoxometalates consist of transition metal oxide polyhedra, may be prepared with different sizes, compositions, nuclearity, structures/architectures, physicochemical properties, and exhibit counterion- and pH-dependent extraordinary self-assembly behavior. Some of the earliest discovered polyoxometalates include the molybdenum-based compound $(NH_4)_3[PMo_{12}O_{40}]$, by Berzelius, in 1826 [17]. Transition metal-oxo moieties exist in a variety of catalytic systems, and, in particular, those based on molybdenum – readily available, relatively low cost metal - may be promising for catalytic oxidation processes [32,33]. In the last couple of decades, polyoxomolybdates possessing zero-, one-, two- and three-dimensional (*n*-D, *n*=0,1,2,3) structures were developed for catalytic oxidation of different types of substrates, e.g. alcohols, cycloalkanes and olefins [23-25,27-29,34]. Ionic oxomolybdenum polynuclear compounds possessing charge-balancing organic cations were effective epoxidation catalysts for the valorisation of biomass-derived olefins, under mild reaction conditions [28,29,35,36].

In this work, one- (1-D) and two dimensional (2-D) ionic polymolybdate hybrid materials (IPH) were explored as catalysts for the liquid phase epoxidation of olefins, such as biomass-derived terpenic and fatty acid methyl ester compounds, at 70 ºC (Scheme 1). The IPHs included: 1-D methylammonium ammonium trimolybdate $[CH_3NH_3{\cdot}NH_4{\cdot}Mo_3O_{10}]$ **1** and bis(3,5-dimethylanilinium) trimolybdate $[Mo_3O_{10}{\cdot}2(NH_3C_6H_3(CH_3)_2)]$ **2**, bis(4-methylanilinium) trimolybdate $[Mo_3O_{10}{\cdot}2(NH_3C_6H_4CH_3)]$ **3**, and 2-D bis(2,5-dimethylanilinium) pentamolybdate $[Mo_5O_{16}{\cdot}2(NH_3C_6H_3(CH_3)_2)]$ **4**, bis(anilinium) pentamolybdate $[Mo_5O_{16}{\cdot}2(NH_3C_6H_5)]$ **5**, bis(4-methylanilinium) pentamolybdate $[Mo_5O_{16}{\cdot}2(NH_3C_6H_4CH_3)]$ **6**, and bis(4-ethylanilinium) pentamolybdate $[Mo_5O_{16}{\cdot}2(NH_3C_6H_4CH_2CH_3)]$ **7**. The structures of the new IPHs **1** and **3** were solved. Systematic characterisation and catalytic studies were carried out to help understand structure-activity relationships, and investigate the catalyst stability in recycling runs.

((Scheme 1 here))

2. Experimental

2.1. Materials and methods

For the syntheses of the molybdenum catalysts, molybdic acid (p.a. > 98%, POCh), acetic acid (99 %, POCh), 2-propanol (> 99.5 %, Chempur), methylamine (≥ 98 %, BASF), 2,5-dimethylaniline (99 %, Aldrich), were obtained from commercial suppliers and used as received. For the catalytic tests, *cis*-cyclooctene (Cy, 95 %, Aldrich), methyl oleate (Ole, 99 %, Aldrich), methyl linoleate (LinOle, 95 %, Alfa Aesar), methyl decanoate (99 %, Aldrich), undecane (> 99 %, Aldrich), *tert*-butylhydroperoxide (*t*bhp, 5.5 M in decane, Sigma–Aldrich), H_2O_2 (30 % aq., Sigma–Aldrich), acetonitrile (99.9 %, Panreac), anhydrous α,α,α-trifluorotoluene (tft, 99.8 %, Aldrich), toluene ((≥99.9 %, Aldrich), 1,2.dichloroethane (≥99 %, Aldrich), diethyl ether (puriss p.≥a., Sigma–Aldrich), pentane (95 %, Carlo Erba) and MoO_3 (≥99.9 %, Analar) were acquired from commercial sources and used as received.

Routine X-ray powder diffraction (XRPD) data were collected at ambient temperature on a Philips Analytical Empyrean diffractometer equipped with a PIXcel 1D detector, with automatic data acquisition (X'Pert Data Collector software v. 4.2) using monochromatized Cu Kα radiation (λ = 1.54178 Å). Intensity data were collected by the step-counting method (step 0.02°), in continuous mode, in the 2θ range 5 - 60°. Attenuated total reflectance (ATR) FT-IR spectra were measured using a Specac Golden Gate Mk II ATR accessory having a diamond top plate and KRS-5 focusing lenses.

Scanning electron microscopy (SEM) images were collected using a Hitachi S4100 microscope operating at 25 kV. Samples were prepared by deposition on aluminium sample holders followed by carbon coating using an Emitech K 950 carbon evaporator.

2.2. Synthesis of the hybrid catalysts

The new hybrids methylammonium ammonium trimolybdate [$CH_3NH_3 \cdot NH_4 \cdot Mo_3O_{10}$] **1** and bis(2,5-dimethylanilinium) pentamolybdate [$Mo_5O_{16} \cdot 2(NH_3C_6H_3(CH_3)_2)$] **4** were synthesized as described in this section. Compounds bis(3,5-dimethylanilinium) trimolybdate [$Mo_3O_{10} \cdot 2(NH_3C_6H_3(CH_3)_2)$] **2**, bis(4-methylanilinium) trimolybdate [$Mo_3O_{10} \cdot 2(NH_3C_6H_4CH_3)$] **3**, 2-D bis(anilinium) pentamolybdate [$Mo_5O_{16} \cdot 2(NH_3C_6H_5)$] **5**, bis(4-methylanilinium) pentamolybdate [$Mo_5O_{16} \cdot 2(NH_3C_6H_4CH_3)$] **6**, bis(4-ethylanilinium) pentamolybdate [$Mo_5O_{16} \cdot 2(NH_3C_6H_4C_2H_5)$] **7**. were synthesised and characterised as in ref. [27]. For the seven compounds, the syntheses were carried out under acidic aqueous phase conditions, using molybdic acid and an organic compound (of the type amine or aniline) as precursors of molybdenum and the constituent cations, respectively.

2.2.1. Methylammonium ammonium trimolybdate **1**

A mixture of molybdic acid (0.01 mol), methylamine (0.0005 mol) and H_2O (10 mL) were thoroughly mixed, placed in thermo-block and kept at 75 ºC for 7 days. The synthesis afforded a white precipitate, which was filtered, washed with 2-propanol and dried in air, at room temperature. Molybdic acid contains ca. 85 % MoO_3 and sufficient ammonium molybdate for synthesizing **1**. Material **1** was obtained with 95 % yield. Anal. Calcd for $CH_3NH_3 \cdot NH_4 \cdot Mo_3O_{10}$ (497.92 g/mol): C, 2.41; N, 5.63; H, 2.02 %. Found: C, 2.37; N, 5.52; H, 1.96 %. Selected FT-IR ATR bands (cm^{-1}) with assignments based on comparisons to literature data for different compounds [37]: ν = 3095m (υO-H,υC-H), 3022m (υO-H,υC-H), 2833vw (υO-H,υC-H), 2758vw, 2462vw, 1662vw, 1624vw, 1589vw, 1520w, 1436sh, 1421s, 1405 sh, 997vw, 895s (υMo-O-Mo), 872s (υMo-O), 864s, 773vw , 648vs (υMo-O), 462-505, 430vw, 390 vw.

2.2.2. Bis(2,5-dimethylanilinium) pentamolybdate **4**

Molybdic acid (0.01 mol) was dissolved in 150 mL water, under reflux. Subsequently, 0.01 mol 2,5-dimethylammonium dissolved in 50 mL acetic acid was added, and the resultant mixture was refluxed for 24 h. A white precipitate was filtered from the hot mixture, washed with 2-propanol and dried in air, at room temperature. Material **4** was obtained with 92 % yield. Anal. Calcd for $Mo_5O_{16}\cdot 2(C_8H_{12}N)$ (692.16 g/mol): C, 19.61; N, 2.86; H, 2.47 %. Found: C, 19.54; N, 2.91; H, 2.58 %. Selected FT-IR ATR bands (cm^{-1}) with assignments based on comparisons to literature data for different compounds [37]: ν = 3047vw (υC-H, υO-H), 2918vw (υC-H, υO-H), 1598vw (δN-H, υC=C), 1562vw (δN-H, υC=C), 1533vw, 1512vw, 1454vw (υC=C), 1301vw (υC-N), 1242vw, 1222vw, 1159vw, 1124vw (δC-H), 945m (υMo-O), 931w, 905m (υMo-O-Mo), 887vw, 852vs (υMo-O), 812s, 757vs (δN-H,γC-H), 671vs (υMo-O), 546vs (δMo-O-Mo), 520sh, 482vw, 463vw, 443m, 428sh, 380s, 363s.

2.3. Thermal stability and structural studies by X-ray powder diffraction

The thermal stability and phase transformations of the IPHs were studied by variable temperature X-ray powder diffraction (XRPD) measurements, under air atmosphere, using a X‘Pert Pro MPD powder diffractometer equipped with a high-temperature chamber (XRK chamber produced by Anton Paar). X-ray data were collected in the temperature range 25-800 °C, and the 2θ range 5-60°.

The crystal structures were determined using a PANalytical X'Pert PRO MPD diffractometer working in Bragg-Brentano geometry; radiation CuKα 1.54187 Å; 2θ in the range 3 - 80°; interpolated step size of 0.02° 2 θ. For **4**, in order to avoid possible texture effects, for final refinement measurements the sample was loaded into a glass capillary (2r = 0.5 mm) and measured in Debye-Scherrer-Hull geometry. The second derivative method and the Sonneveld-Visser program were used to determine the peak positions in diffraction patterns. The unit cell parameters were obtained using the PROSZKI package [38]. Structure solution for **1** was performed using EXPO-2014 program [39] working in direct methods mode; and program FOX [40] applying direct space methods (global optimization, variant: parallel tempering) was used for **4**. Restrained Rietveld refinement was carried out using the Jana2006 program [41]. The shape of the diffraction lines in both cases was described by pseudo-Voigt function, the background was described by the Legendre polynomials (no. terms 15). Rietveld refinement plots are given in the Supplementary Information section (SI): SI-Fig. 1 and SI-Fig. 2.

2.4. Catalytic tests

The IPH catalysts were tested for the epoxidation the olefins methyl oleate (Ole), methyl linoleate (LinOle), R-(+)-limonene (Lim), and *cis*-cyclooctene (Cy), using *tert*-butylhydroperoxide (*t*bhp) as oxidant, and α,α,α-trifluorotoluene (tft) as solvent. Hydrogen peroxide was used (for selected catalytic system) as oxidant instead of *t*bhp, with acn as cosolvent allowing the miscibility of the substrate and oxidant. For the reaction of Ole with *t*bhp, different cosolvents were tested, namely, 1.2-dichloroethane (dce), toluene (tol), and acetonitrile (acn), besides tft. The catalytic reactions were carried out in 10 mL borosilicate reactors equipped with a Teflon valve (for sampling) and a magnetic stirrer. The reactor was loaded with catalyst (18 μmol Mo), co-solvent (1 mL) and olefin (1.8 mmol), and then immersed in a temperature-controlled oil bath at 55 or 70 °C, under stirring (1000 rpm), for 10 min. The oxidant (2.75 mmol for Cy, Lim and Ole, and 2.75 mmol or 4.80 mmol for MeOle reactions) was pre-heated in a separate flask for 10 min at the same temperature, and then added to the reactor. The instant that the pre-heated oxidant was added to the reactor was taken as the initial instant of the catalytic reaction. The reaction mixtures were analyzed using a Varian 3900 GC equipped with a DB-5 capillary column (30 m × 0.25 mm × 0.25 μm) and a FID detector, with H_2 as the carrier gas, and quantifications were based on calibrations. The internal standards used were undecane for the Cy and Lim reactions, and methyl decanoate for the Ole and LinOle reactions. The experimental range of error was less than 6 %, based on replicates carried out for selected experimental conditions. The material balance considering all reaction products quantified by GC closed in: 100 % for Cy at 24 h reaction, 100 % for Ole at 6 h, 98 % for Lime and 98 % LinOle at 24 h reaction, 70 ºC. The reaction products were identified by GC–MS (Trace GC 000 Series Thermo Quest CE Instruments GC; Thermo Scientific DSQ II), using He as the carrier gas. The product identifications were based on commercial mass spectrometry databases (Wiley6, NIST2.0, NIST Chemistry WebBook, MAINLIB), and mass spectral matching data.

After each 24 h batch run (Cy reaction), the IPHs were separated from the reaction mixtures by centrifugation (3500 rpm), thoroughly washed with diethyl ether/pentane, dried overnight under atmospheric conditions, and finally vacuum-dried (ca. 4 bar) at 60 °C for 1 h. The initial mass ratios of olefin/oxidant/metal compound were the same for all batch runs. The solids recovered from the first and second batch runs are denoted as (**i**)-run1 and (**i**)-run2, respectively, where **i** = **1**-**7**. The recovered molybdenum compounds were characterized by ATR FT-IR spectroscopy, XRPD and SEM.

The homogeneous or heterogeneous nature of the catalytic reaction was studied by carrying out a contact test (ct). Specifically, **2** and the benchmark catalysts MoO_3 and molybdic acid were mixed with the oxidant and solvent, under similar conditions to those used for a normal catalytic test, but without substrate, for 24 h, at 70 °C, with stirring. The obtained mixture was heterogeneous (biphasic solid-liquid, containing oxidant, solvent, and solid molybdenum compound), and was cooled to ambient temperature. The solid compound was separated from the liquid phase by passing the heterogeneous mixture through a filter equipped with a 0.2 µm PTFE membrane, giving the solution **2**-L-ct. Then, the substrate Cy (preheated to 70 °C) was added to the solution **2**-L-ct in an amount to give an initial Cy concentration of 1.2 M (similar to that used for a normal catalytic test); the resultant solution (a homogeneous liquid) was stirred for 24 h, at 70 °C, and analysed by GC to check if the epoxidation reaction occurred in homogeneous phase.

The oxidant efficiency was determined by iodometric titration for **2**. After a 24 h catalytic batch run at 70 ºC, the reaction mixture was cooled to ambient temperature, and liquid samples were withdrawn for titration. The experimental range of error was 5-10 %, based on replicates.

The structure-activity relationships were based on initial catalytic activity (or initial turnover frequency) calculated for 1 h reaction, for which catalyst deactivation may be neglected.

3. Results and Discussion

3.1. Crystal structures

Material **1** belongs to the group of trimolybdate type IPHs, their characteristic feature being an infinite polymeric 1-dimensional (1-D) chain of $Mo_3O_{10}^{2-}$ anions (Tables 1 and 2, SI-Fig. 1). The crystal structure of **1** is reflected in its morphological features, i.e. the crystallites of **1** are thin needles (ca. 300-400 nm thick) (SI-Fig. 3.a). The anions are surrounded by methylammonium and ammonium cations; the latter are connected with anions by ionic interactions and a system of H-bonds (Figure 1). The chains are built of edges and vertices shared by deformed MoO_6 octahedra (Figure 1). Two MoO_6 octahedra, by sharing one edge, form dimers Mo_2O_{10}. Such dimers, in turn, by sharing two upper and two lower vertices with identical dimers form infinite ribbons with the formula Mo_2O_8. To the ribbons, alternately from both sides, are attached MoO_6 octahedra. In this way, infinite zigzag chains are obtained with the general formula $Mo_3O_{10}^{2-}$. Polymeric anions are aligned parallel to the b axis. In each MoO_6 octahedron there are two terminal oxygen atoms in *cis* position to each other and four μ_3-O atoms. In a similar fashion, several trimolybdate type IPHs are built, including methylammonium trimolybdate, potassium, ammonium, silver, anilinium or 3,5-dimethylanilinium trimolybdate [27]. The longer distance between the chains of **1** is 9.569 Å, and for the 1-D materials **2** and **3** it is 16.79 and 15.15 Å, respectively (SI-Fig. 5).

((Figure 1 and Tables 1 and 2 here))

The IPH **4** crystallises as very fine, thin plates (SI-Fig. 3.b) and is built in similar fashion to the remaining layered pentamolybdate type IPHs (Figure 2, Tables 1 and 3, SI-Fig. 6). Material **4** possesses parallel layers overlapping with crystallographic planes (200). The interplanar d-spacing d(200) for **4** is 17.22 Å (SI-Fig. 6.a), and for the 2-D materials **5, 6** and **7** it is 13.60, 14.36 and 15.15 Å, respectively (SI-Fig. 6.b,c,d). Infinite, staggered layers built of distorted MoO_6 octahedra sharing edges and corners, form an open-framework (Figure 2, Tables 1 and 3). In each asymmetric unit there are three Mo atoms, 8 oxygen atoms and one 2,5-dimethylanilinium cation. Due to the relative spatial arrangement of the methyl substituents, in order to compensate the negative charge of the anionic layers, the 2,5-dimethylanilinium cations form double layers of cations between anionic layers. As a result, the interplanar d-spacing d(200) is greater for **4** than the anilinium **5**, 4-methylanilinium **6**, or 4-ethylanilinium **7** pentamolybdates [27].

((Figure 2 and Table 3 here))

3.2. Thermal stability

The variable temperature XRPD studies indicated that the 1-D IPH **1** is stable up to 225 °C, and further increase of the temperature led to the formation of a 3-D material with a system of infinite, parallel, hexagonal channels (SI-Fig. 4.a). The obtained non-stoichiometric compound, the so-called hexagonal molybdenum oxide (PDF-4+: 048-0399), consists of channels intercalated by small cations (e.g. Na^+, K^+), which, for **4**, are ammonium or methylammonium cations. The amount of cations may depend on the temperature or synthesis conditions. Further heating to ca. 300 °C led to the formation of stoichiometric, layered MoO_3 (PDF-4+: 35-609). Similar behaviour was reported in the literature for ammonium heptamolybdate tetrahydrate [42]. The IPH **3** is stable up to ca. 200 °C; in the range 225-300 °C it is transformed into an amorphous phase, and at ca. 350 °C, layered MoO_3 is formed (PDF-4+: 35-609) (SI-Fig. 4.b). Materials **1** and **4** are thermally stable at the catalytic reaction temperature of 70 °C. The same applies for **2**, **3**, **5**-**7**, based on thermal stability studies reported in the literature by some of us [27].

3.3. Catalytic studies

3.3.1. General considerations

The new IPHs methylammonium ammonium trimolybdate [$CH_3NH_3 \cdot NH_4 \cdot Mo_3O_{10}$] **1** and bis(2,5-dimethylanilinium) pentamolybdate [$Mo_5O_{16} \cdot 2(C_6H_3NH_3(CH_3)_2)$] **4** possess the same structure as **2**/**3** (1-D trimolybdate moities) or **5-7** (2-D pentamolybdate moieties), respectively. Systematic catalytic and characterisation studies were carried out in order to help gain insights into structure-activity relationships, and catalyst stability. For these studies, *cis*-cyclooctene (Cy) was used as model substrate, *tert*-butyl hydroperoxide (*t*bhp) as oxidant. α,α,α-Trifluorotoluene (tft) was chosen as solvent, since it is hydrophobic, avoiding negative effects of moisture, for example, on epoxide selectivity [29,35,43], and a non-coordinating solvent, avoiding competitive effects between the solvent and reactant molecules for the coordination to the metal centres (based on mechanistic considerations discussed ahead) [44]. For all catalysts investigated, 1,2-cyclooctene epoxide (CyO) was formed in 100 % selectivity, and 97-100 % CyO yield, at 70 °C/24 h (Table 4). Without catalyst and/or oxidant, the reaction was very sluggish (< 7 % CyO yield at 70 °C/24 h) [43].

The highest catalytic activity was observed for **2** and **3**, which led to 97 and 100 % CyO yield, respectively, at 1 h (turnover frequency (TOF) = 97 or 100 mol mol_{Mo}^{-1} h^{-1}), compared to 24-54 % yield (TOF in the range 24-54 mol mol_{Mo}^{-1} h^{-1}) for the remaining compounds (Table 4). For **2** and **3**, decreasing the reaction temperature from 70 to 55 °C, led to a decrease in initial activity from 97 to 71 mol mol_{Mo}^{-1} h^{-1} for **2**, and from 100 to 91 mol mol_{Mo}^{-1} h^{-1} for **3** (Table 4). Nevertheless, quantitative CyO yield was reached within 6 h reaction for these two catalysts, at 55 °C. Clear, fair comparisons of the catalytic results to literature data are not trivial due to the different reaction conditions used between different works. A literature survey for polyoxomolybdates and the model reaction Cy/*t*bhp, under similar reaction conditions (Table 5, [45-53]), indicated that **2** and **3** performed superiorly in relation to e.g. $(H_3biim)_4[\beta\text{-}Mo_8O_{26}]$ where H_2biim = 2,2'-biimidazole [29], and $[\{MoO_2(HC(3,5\text{-}Me_2pz)_3)\}_2(\mu_2\text{-}O)][Mo_6O_{19}]$ where $HC(3,5\text{-}Me_2pz)_3$ = tris(3,5-dimethyl-1-pyrazolyl)methane [30].

((Tables 4 and 5 here))

3.3.2. Catalyst stability and benchmarking

The reaction mixtures were biphasic solid-liquid, for **1**-**7**. After the catalytic reaction at 70 °C, the used catalyst was characterised, and reused in consecutive catalytic batch runs (details given in the experimental section). The used catalysts are denoted (**i**)-runx, where i is referent to compounds **1**-**7**, and x = 1 and 2 for the solids recovered from the batch runs 1 and 2, respectively. For each IPH, excluding **3**, the catalytic results were somewhat comparable in consecutive batch runs (Figure 3). The characterisation studies for **1**, **2**, **4**-**7** indicated somewhat comparable results for the original and respective used catalyst. Hence, the chemical (based on FT-IR ATR spectroscopy, Figures 4 and 5), structural (XRPD, Figures 4 and 6) and morphological (SEM, Figure 6) features were essentially preserved during the catalytic process using **1**, **2**, **4**-**7**. For **3**, Cy conversion decreased somewhat considerably from the first to the third run, suggesting that this catalyst was less stable (Figure 3). The used catalyst exhibited a different FT-IR ATR spectrum, XRPD pattern (amorphous material) and morphology (based on SEM) from the respective original catalyst **3** (SI-Fig. 7). Overall, the best-performing catalyst in terms of activity and stability was the IPH **2**.

For the best-performing catalyst **2**, a contact test (ct) was carried out in order to study the homogeneous or heterogeneous nature of the catalytic reaction (details in the experimental section). The solution obtained from the ct (**2**-L-ct) was tested for the homogeneous catalytic reaction of Cy, and gave ca. 28 % conversion at 24 h. This result is far poorer than that for the original catalyst **2** (97 % at 1 h), suggesting that the catalytic contribution of the dissolved molybdenum species was relatively small, and thus the activity is mainly attributed to the solid-state catalyst.

For comparison, commercial MoO_3 and molybdic acid (denoted MoAc) were tested as catalysts, under similar Cy reaction conditions to those used for **2** (Table 5). The commercial catalysts led to much slower Cy reaction, at 70 ºC: for MoO_3, 4 %/71 % conversion, at 1 h/6 h (CyO yield was equal to conversion), and for MoAc, 4 %/96 % conversion and 4 %/96 % CyO yield, at 1 h/6 h, whereas **2** led to 97 % conversion at 1 h. On the other hand, MoO_3 and MoAc presented considerable homogeneous catalytic contributions, ascertained by the corresponding ct. Specifically, the liquid phase (MoO_3-L-ct) of the ct for MoO_3 was tested for the reacion of Cy (in a similar fashion to that described for **2**), and gave 76 % conversion at 24 h, which is considerable in relation to that for the normal catalytic test (without filtration of the solid) in the presence of MoO_3 (96 % conversion at 24 h, Table 5). Likewise, the liquid phase (MoAc-L-ct) of the ct for MoAc was tested for the reacion of Cy, and gave 100 % conversion at 24 h, which is similar to that for the normal catalytic test using MoAc (100 % conversion at 24 h, Table 5).

((Figures 3, 4, 5 here))

3.3.3. Structure-activity relationships

The IPHs **1**-**7** possess an organic cationic component, and an inorganic anionic scaffold consisting of corner and edge sharing Mo(VI)O_6 octahedra, which are assembled to give

1-D structures (trimolybdate type IPHs **1**-**3**) or 2-D structures (pentamolybdate type IPHs **4**-**7**). Compounds **1-7** may be compared in two perspectives. One the one hand, a comparison based on the nature of the organic part clearly shows that the anilinium-based IPHs were more active than aliphatic amine-based IPH (Table 4). On the other hand, the family of anilinium-based catalysts, which is more extensive, is interesting for more detailed comparisons. A comparative study for the group of anilinium-based IPHs **2**-**7**, suggested that the type of substituents of the aniline ring may influence the crystalline structure. For example, while the 3,5-dimethyl substitution led to the 1-D trimolybdate **2**, the 2,5-dimethyl substitution led to the 2-D pentamolybdate **4**. On the other hand, the synthesis conditions influence the structural features of the IPHs. For example, depending on the temperature, time and acidic conditions, the syntheses using the same precursor of bis(4-methylanilinium) gave the structurally different IPHs **3** and **6** [27]. In order to gain insights into structure-activity relationships, the catalytic performances were compared on the basis of initial activity. Figure 7.a compares the initial activity for the 1-D versus 2-D structures, and Figure 7.b shows the initial activity versus the distances between chains/layers for the anilinium-based IPHs. The results suggest more significant influence of the structure dimensionality (Figure 7.a) than the distance between chains/layers (Figure 7.b) on the catalytic performances. The initial catalytic activity (mol $\text{mol}_{\text{Mo}}^{-1}$ h^{-1}) followed the order **6** (40) < **7** (44) < **5** (48) < **4** (54) << **2** (97) < **3** (100) (Table 4). The 1-D IPHs **2** and **3** were far more active than the 2-D **4-7** ones. For example, the anilinium-based IPHs **2** and **4**, which possess 1-D and 2-D structures, respectively, and comparable distances between chains/layers (16.79 and 17.22 Å, respectively), it was verified that the 1-D catalyst was far more active than the 2-D one. On the other hand, a comparitive study of **2** and **3** (1-D structures) indicated that while the disubstituted anilinium possessed longer distance between chains than the monosubstituted one, initial activity was comparable for the two IPHs (Figure 7.b). The same applies when comparing **6** and **7** (2-D structures) in that a substituent group with a longer carbon chain (4-methyl versus 4-ethyl) led to enlarged interplanar distance of the IPH, but did not affect significantly the initial activity. Moreover, the unsubstituted anilinium (5) possessed the smallest interplanar distance of the 2-D catalysts, and its initial activity was comparable to those of the remaining 2-D catalysts. These comparisons support the above hypothesis in that the structure dimensionality of the anilinium-based IPHs is an important factor influencing the catalytic activity.

Hence, the catalytic activity seems favoured by a lower structure dimensionality. Similar effects were reported in the literature for (non-ionic) molybdenum-triazole hybrids [54,55].

In order to help understand the influence of the structure on the catalytic activity, it is important to take into consideration the reaction mechanism involved. The reaction mechanism of olefin epoxidation with hydroperoxide oxidants, in the presence of molybdenum catalysts, may involve the coordination of the hydroperoxide molecules to the metal centre, giving an active oxidising species responsible for the O-atom transfer to the olefin, which finally leads to the formation of epoxide product [56,57]. Since the organic cations are in the acidic form (protonated), their influence on the Lewis acidity of the metal centres (active sites) may be less important than the structural features. For 1-D structures, the active sites may be more accessible, and the interactions of the reactant molecules with the metal centres may be less hindered, than for the 2-D structures, favouring the reaction kinetics.

((Figures 6 and 7 here))

3.3.4. Catalytic conversion of biomass-derived olefins

The best-performing catalyst **2** was studied for the catalytic epoxidation of the bio-derived FAMEs methyl oleate (Ole) and methyl linoleate (LinOle), which are, readily available in nature (canola, soybean, sunflower and corn oils, for example), Scheme 1 [58]. The system Ole/**2**/*t*bhp gave methyl 9,10-epoxyoctadecanoate (OleOx) as the main product formed in 48/84/92 % yield, at 51/89/99 % conversion (0.5 h/6 h/24 h), 70 °C (Figures 8 and 9.a). Methyl 9,10-dihydroxyoctadecanoate (OleOH) and methyl 9-oxooctadecanoate were formed in yields of 4 and 3 %, respectively, at 24 h.

The fatty acid methyl ester LinOle possesses two double bonds C=C, and thus the LinOle reaction was carried out using a molar ratios substrate:oxidant of 1.5 or 2.5, in the presence of **2** (Figures 8 and 9.b). Monoepoxide products, namely methyl 9,10-epoxy-12-octadecenoate and methyl 12,13-epoxy-9-octadecenoate (LinOleOx isomers) were formed with 60 % total yield (at 72 % conversion, 2 h reaction). LinOleOx selectivity decreased with reaction time greater than 2 h, which was accompanied by the formation of (diepoxide) methyl 9,10-12,13-diepoxyoctadecanoate (LinOleDiox) and cyclization products (e.g. methyl 10,13-epoxy-9,12-dihydroxyoctadecanoate). These results suggest that LinOleOx is an intermediate of the conversion of LinOle to LinOleDiox and cyclization products, in agreement with the literature [59]. For the molar ratios LinOle:*t*bhp of 1.5 or 2.5, the LinOle reaction kinetics was similar (Figure 8), albeit the higher amount of *t*bhp seems to favour the formation of LinOleDiox and cyclization products (Figure 8.b); it was reached 36-39 % LinOleOx, 28-39 % LinOleDiox yield, and 16-28 % yield of cyclization products, at 94-95 % conversion.

((Figures 8 and 9 here))

Compound **2** was tested for the epoxidation of R-(+)-limonene (Lim), the most abundant limonene isomer present in citrus oil, at 70 °C (Scheme 1). The reaction was fast, and gave mainly 1,2-epoxy-*p*-menth-8-ene (LimOx) formed in 71 %/76 % yield, at 83 %/96 % conversion (and 1 h/4 h) (Figures 8 and 10). Besides LimOx, it was formed 1,2:8,9-diepoxy-*p*-menthane (LimDiOx) and 1-methyl-4-(1-methylethenyl)-1,2-cyclohexanediol (LimDiOH) (5 %/10 % and 2 %/7 % yield, respectively, at 1 h/4 h).

To the best of our knowledge, **2** is the first IPH catalyst studied for (i) LinOle epoxidation and (ii) Lim reaction with *t*bhp (also, no polyoxomolybdates were reported as catalysts for the reaction system Lim/*t*bhp). Few studies were reported in the literature for polyoxomolybdate-catalysed epoxidation of Ole. The compounds $(C_5H_5NH)_4[Mo_8O_{26}]$ and $[(CH_3)_3CC_5H_4NH]_4[Mo_8O_{26}]$ led to ca. 99 % OleOx yield, at 6 h, 75 ºC (initial molar ratio Mo:Ole:*t*bhp=1:100:152; dce as co-solvent) [28]; at lower reaction temperature (70 ºC), **2** led to 89 % OleOx yield, at 6 h. Under similar reaction conditions (time, temperature) to those used for **2**, the compound $(H_3biim)_4[\beta\text{-}Mo_8O_{26}]$ (H_2biim = 2,2'-biimidazole) led to 64 % OleOx yield at 24 h, 70 °C (initial molar ratio Mo:Ole:*t*bhp=1:100:152; ionic liquid as co-solvent) [29]; in comparison to these results, **2** performed superiorly (92 % OleOx yield). Iodometric titration indicated approximately 100 % *t*bhp efficiency, i.e. the catalyst does not account for a measurable non-productive decomposition of *t*bhp to molecular oxygen plus tert-butanol.

The influence of the temperature on the reaction of Ole with *t*bhp was studied in the range 55-85 ºC. Increasing the temperature led to faster reaction of Ole to OleOx; 19, 66 and 81 % OleOx yield at 1 h for the reaction temperature of 55, 70 and 85 ºC, respectively (Table 6). Approximately the same OleOx yield was reached at 6 h/85 ºC (89 %) and 24 h/70 ºC (92 %).

The influence of the type of solvent (can, tft, dce, tol) on the Ole/*t*bhp reaction at 70 ºC was studied (Table 6). The most significant difference in catalytic results was the much slower initial reaction (based on conversion at 1 h, Table 6) for acn than the remaining cosolvents. The cosolvent acn is more polar than the remaining ones, albeit no direct relationship between the solvent polarity and the initial reaction rate could be established. Based on the normalized spectroscopically derived empirical scale of solvent polarity (adimensional E^N_T, ranging from 0.000 for apolar tetramethylsilane to 1.000 for (most polar) water [60]), the solvent polarity follows the order, tol (0.099) < tft (0.241) < dce (0.327) < acn (0.460), whereas conversion at 1 h follows the order, acn (31 %) << tol (63 %) < tft (70 %) ≈ dce (71 %). An important characteristic that distinguishes acn from the remaining cosolvents is its coordinating ability. While acn is an aprotic coordinating cosolvent, the remaining cosolvents tft, dce and tol are non-coordinating. Thus, the slower kinetics for acn may be partly due to competitive effects between the solvent and oxidant molecules in the coordination to the molybdenum species, retarding the overall catalytic reaction [61-65].

((Table 6 here))

The IPH catalyst **2** was further studied for Ole conversion using H_2O_2 as oxidant instead of *t*bhp. Iodometric titration indicated 98 % H_2O_2 efficiency for the catalytic epoxidation system. Hence, **2** enables very efficient use of the peroxide oxidants for catalytic epoxidation. However, in relation to the reaction of Ole with *t*bhp, the catalyst was poorly effective with H_2O_2 (13 % conversion at 24 h). According to the literature, the transition state involved in the epoxidation reaction may differ for alkyl hydroperoxides versus hydrogen peroxide as oxidant, affecting the reaction kinetics [66-72]. Nevertheless, *t*bhp is an interesting oxidant, since its use for catalytic epoxidation presents as possible advantages relatively safe transportation, storage, handling, and it is miscible with many organic solvents [73], being the oxidant of choice for epoxidation processes by industries, e.g. LyondellBasell [74] and Huntsman processes [75].

IPHs are versatile materials in that the type of transition metal and organic precursor may be changed, which may lead to different performances. For example, it is possible that tungsten-based IPHs may promote the one-pot epoxidation-hydrolysis of bio-olefins to useful diols (e.g. intermediates to producing oleo-chemical based renewable polymers). Kozhevnikov et al. [76] reported the reaction of oleic acid with H_2O_2 in the presence of a peroxophosphotungstate homogeneous catalyst, which led to the corresponding diol product in 61 % yield at 93 % conversion (80 ºC, 160 min); decreasing reaction temperature and time (60 ºC, 50 min) led to the epoxide as the main product formed in 84 % yield at 95 % conversion. Later Poli et al. [77] reported the immobilisation of peroxophosphotungstate on mesoporous silica SBA-15, as heterogeneous catalyst for the reaction of Ole with H_2O_2, at 65 ºC; this catalyst was not effective in the first batch run, but it was suggested that favourable changes in geometry of the polyanion occurred during the first run, which led to superior results in the second run (4 % and 44 % epoxide yield at 15 h. for runs 1 and 2, respectively). Very recently, it was reported that ionic organic-inorganic polyoxotungstates are capable of promoting the oxidative cleavage of fatty acids, at relatively high temperature (120 ºC); specifically, the reaction oleic acid/H_2O_2 gave azelaic (C9 diacid) and pelargonic (C9 monoacid) acids, which are industrially produced from oleic acid via ozonolysis (use of hazardous ozone) [78]. IPHs, besides being versatile materials, may possess relatively high thermal stability (~200 ºC [27]) for these catalytic applications.

((Figure 10 here))

Conclusions

Ionic polymolydate hybrids **1-7** were prepared in simple and relatively clean fashions, and are effective olefin epoxidation catalysts. Catalyst stability and characterization studies (FT-IR ATR spectroscopy, XRPD, SEM) of the used catalysts, indicated fairly steady performances in consecutive batch runs, and the chemical, structural and morphological features of the materials were essentially preserved. The type of synthetic organic precursor and synthesis conditions influence the structural features of the IPHs, with structure dimensionality (1-D, 2-D) impacting on the catalytic activity. The best-performing catalyst **2** (in terms of activity and stability) possesses a 1-D structure. The IPH **2** was effective for the conversion of biomass-derived olefins, specifically, fatty acid methyl esters (methyl oleate (Ole), methyl linoleate (LinOle)) and terpene (limonene) to bio-products; e.g. Ole was converted to the corresponding epoxide methyl 9,10-epoxyoctadecanoate in 92 % yield, at 70 °C/24 h (approximately atmospheric pressure). The reaction kinetics seemed favoured by increasing the reaction temperature and using non-ccordinating cosolvents. To the best of our knowledge, this is the first report of LinOle epoxidation, and Lim/*t*bhp conversion in the presence of IPH catalysts.

Ionic polymetallate hybrids are versatile materials; by changing the type of transition metal and organic precursor, their applications may be broadened to different types of catalytic reactions, and different scientific fields.

Acknowledgments

This work was developed in the scope of the project CICECO – Aveiro Institute of Materials [POCI-01-0145-FEDER-007679] financed by national funds through the Fundação para a Ciência e a Tecnologia (FCT) [ref. UID/CTM/50011/2013] and Ministério da Educação e Ciência (MEC) and when applicable, cofinanced by Fundo Europeu de Desenvolvimento Regional (FEDER) under the PT2020 Partnership Agreement. The FCT and the European Union are acknowledged for a post-doctoral grant to P.N. [SFRH/BPD/110530/2015], cofunded by Ministério da Ciência, Tecnologia e Ensino Superior (MCTES) and the European Social Fund through the program Programa Operacional Potencial Humano (POPH) of Quadro de Referência Estratégica Nacional (QREN). The European Union Erasmus+ programme [project number: 2016-1-PL01-KA103-023786] is acknowledged for providing scholarship (financial support) for the traineeship (B.B).

References

[1] P. Muturi, D. Q. Wang, S. Dirlikov, Prog. Org. Coat. 25 (1994) 85-94.

[2] N. O. Shaker, E. M. Kandeel, E. E. Badr, M. M. El-Sawy, J. Dispersion Sci. Technol. 29 (2008) 421-425.

[3] S. F. Thames, H. Yu, Surf. Coat. Technol. 115 (1999) 208-214.

[4] K. M. Doll, S. Z. Erhan, J. Surfactants Deterg. 9 (2006) 377-383.

[5] A. Adhvaryu, S. Z. Erhan, Ind. Crops Prod. 15 (2002) 247-254.

[6] K. M. Doll, B. R. Moser, S. Z. Erhan, Energy Fuels 21 (2007) 3044-3048.

[7] E. Milchert, K. Malarczyk, M. Klos, Molecules, 20 (2015) 21481-21493.

[8] A. J. Bonon, Y. N. Kozlov, J. O. Bahu, R. Maciel Filho, D. Mandelli, G. B. Shul'pin, J. Catal. 319 (2014) 71-86.

[9] A. Corma, S. Iborra, A. Velty, Chem. Rev. 107 (2007) 2411-2502.

[10] C. L. Li, S. van Berkel, R. J. Sablong, C. E. Koning, Eur. Polym. J. 85 (2016) 466-477.

[11] R. C. Jeske, A. M. DiCiccio, G. W. Coates, J. Am. Chem. Soc. 129 (2007) 11330-11331.

[12] P. A. Wilbon, F. Chu, C. Tang, Macromol. Rapid Commun. 34 (2013) 8-37.

[13] M. Baehr, A. Bitto, R. Muelhaupt, Green Chem. 14 (2012) 1447-1454.

[14] C. L. Li, R. J. Sablong, C. E. Koning, Angew. Chem. Int. Ed. 55 (2016) 11572-11576.

[15] C. Martin, A. W. Kleij, Macromolecules, 49 (2016) 6285-6295.

[16] M. Guidotti, R. Psaro, I. Batonneau-Gener, E. Gavrilova, Chem. Eng. Technol. 34 (2011) 1924-1927.

[17] L. Cronin, A. Muller, Chem. Soc. Rev. 41 (2012) 7333-7334.

[18] J. M. Clemente-Juan, E. Coronado, A. Gaita-Arino, Chem. Soc. Rev. 41 (2012) 7464-7478.

[19] H. J. Lv, Y. V. Geletii, C. C. Zhao, J. W. Vickers, G. B. Zhu, Z. Luo, J. Song, T. Q. Lian, D. G. Musaev, C. L. Hill, Chem. Soc. Rev. 41 (2012) 7572-7589.

[20] C. Streb, Dalton Trans. 41 (2012) 1651-1659.

[21] P. C. Yin, D. Li, T. B. Liu, Chem. Soc. Rev. 41 (2012) 7368-7383.

[22] B. Bujanovic, S. Ralph, R. Reiner, K. Hirth, R. Atalla, Materials 3 (2010) 1888-1903.

[23] J. Du, J. Yu, J. Tang, J. Wang, W. Zhang, W. R. Thiel, M. Jia, Eur. J. Inorg. Chem. (2011) 2361-2365.

[24] T. Okuhara, N. Mizuno, M. Misono, Appl. Catal. A-Gen. 222 (2001) 63-77.

[25] I. V. Kozhevnikov, Chem. Rev. 98 (1998) 171-198.

[26] H. Yanagie, A. Ogata, S. Mitsui, T. Hisa, T. Yamase, M. Eriguchi, Biomed. Pharmacother. 60 (2006) 349-352.

[27] A. Szymanska, W. Nitek, M. Oszajca, W. Lasocha, K. Pamin, J. Poltowicz, Catal. Lett. 146 (2016) 998-1010.

[28] C. A. Gamelas, P. Neves, A. C. Gomes, A. A. Valente, C. C. Romão, I. S. Gonçalves, M. Pillinger, Catal. Lett. 142 (2012) 1218-1224.

[29] P. Neves, T. R. Amarante, A. A. Valente, M. Pillinger, I. S. Goncalves, Catal. Lett. 146 (2016) 841-850.

[30] A. C. Gomes, P. Neves, S. Figueiredo, J. A. Fernandes, A. A. Valente, F. A. Almeida Paz, M. Pillinger, A. D. Lopes, I. S. Gonçalves, J. Mol. Catal. A: Chem. 370 (2013) 64-74.

[31] M. Najafi, A. Abbasi, M. Masteri-Farahani, V. H. Rodrigues, J. Sci., Islamic Repub. Iran 25 (2014) 229-235.

[32] H. Arzoumanian, Coord. Chem. Rev. 178 (1998) 191-202.

[33] R. Sanz, M. R. Pedrosa, Curr. Org. Synth. 6 (2009) 239-263.

[34] A. Kumar, A. K. Gupta, M. Devi, K. E. Gonsalves, C. P. Pradeep, Inorg. Chem. 56 (2017) 10325-10336.

[35] T. R. Amarante, P. Neves, A. A. Valente, F. A. Almeida Paz, A. N. Fitch, M. Pillinger, I. S. Gonçalves, Inorg. Chem. 52 (2013) 4618-4628.

[36] B. M. Trost, Y. Masuyama, Isr. J. Chem. 24 (1984) 134-143.

[37] M. Oszajca, N. Juszczyk, W. Lasocha, J. Mol. Struct. 965 (2010) 131-136.

[38] W. Lasocha, K. Lewiński, J. Appl. Cryst. 27 (1994) 437-438.

[39] A. Altomare, M. Camalli, C. Cuocci, C. Giacovazzo, A. Moliterni, R. Rizzi, J. Appl. Cryst. 42 (2009) 1197-1202.

[40] V. Favre-Nicolin, R. Cerny, J. Appl. Cryst. (2002) 734-743.

[41] V. Petricek, M. Dusek, L. Palatinus, Jana 2006. The crystallographic computing system, 2006, Institute of Physics, Czech Republic.

[42] J. Wienold, R. E. Jentoft, T. Ressler, Eur. J. Inorg. Chem. (2003) 1058-1071.

[43] P. Neves, L. S. Nogueira, A. C. Gomes, T. S. M. Oliveira, A. D. Lopes, A. A. Valente, I. S. Goncalves, M. Pillinger, Eur. J. Inorg. Chem. (2017) 2617-2627.

[44] T. R. Amarante, P. Neves, C. Tomé, M. Abrantes, A. A. Valente, F. A. Almeida Paz, M. Pillinger, I. S. Gonçalves, Inorg. Chem. 51 (2012) 3666-3676.

[45] H. C. Gao, J. H. Yu, J. Du, H. L. Niu, J. Wang, X. J. Song, W. X. Zhang, M. J. Jia, J. Cluster Sci. 25 (2014) 1263-1272.

[46] M. Najafi, A. Abbasi, M. Masteri-Farahani, H. Shahbaazi, M. A. Motlagh, J. Janczak, RSC Adv. 6 (2016) 29944-29949.

[47] S. Y. Li, C. W. Kee, K. W. Huang, T. S. A. Hor, J. Zhao, Organometallics 29 (2010) 1924-1933.

[48] J. Pisk, B. Prugovecki, D. Matkovic-Calogovic, T. Jednacak, P. Novak, D. Agustin, V. Vrdoljak, RSC Adv. 4 (2014) 39000-39010.

[49] M. Ghorbanloo, R. Bikas, G. Malecki, Inorg. Chim. Acta 445 (2016) 8-16.

[50] C. Bhaumik, E. Manoury, J.-C. Daran, P. Soezen-Aktas, F. Demirhan, R. Poli, J. Organomet. Chem. 760 (2014) 115-123.

[51] B. Zhang, S. Li, A. Pothig, M. Cokoja, S. L. Zang, W. A. Herrmann, F. E. Kühn, Z. Naturforsch., B: Chem. Sci., 68 (2013) 587-597.

[52] M. Moghadam, V. Mirkhani, S. Tangestaninejad, I. M.-Baltork, M. M. Javadi, Polyhedron 29 (2010) 648–654.

[53] M. Moghadam, V. Mirkhani, S. Tangestaninejad, I. M.-Baltork, M. M. Javadi, Inorg. Chem. Commun. 13 (2010) 244–249.

[54] A. B. Lysenko, G. A. Senchyk, K. V. Domasevitch, J. r. Hauser, D. Fuhrmann, M. Kobalz, H. Krautscheid, P. Neves, A. A. Valente, I. S. Gonçalves, Inorg. Chem. 54 (2015) 8327-8338.

[55] A. B. Lysenko, G. A. Senchyk, K. V. Domasevitch, M. Kobalz, H. Krautscheid, J. Cichos, M. Karbowiak, P. Neves, A. A. Valente, I. S. Gonçalves, Inorg. Chem. 56 (2017) 4380-4394.

[56] L. F. Veiros, A. Prazeres, P. J. Costa, C. C. Romão, F. E. Kühn, M. J. Calhorda, Dalton Trans. (2006) 1383-1389.

[57] F. E. Kühn, M. Groarke, E. Bencze, E. Herdtweck, A. Prazeres, A. M. Santos, M. J. Calhorda, C. C. Romão, I. S. Gonçalves, A. D. Lopes, M. Pillinger, Chem. Eur. J. 8 (2002) 2370-2383.

[58] Nikesh B. Samarth, P. A. Mahanwar, Open J. Org. Polym. Mater. 5 (2015) 1-22.

[59] G.J. Piazza, A. Nuñez, T. A. Foglia, J. Am. Oil Chem. Soc. 80 (2003) 901-904.

[60] C. Reichardt, Chem. Rev. 94 (1994) 2319-2358.

[61] W. R. Thiele, J. Mol. Catal. A: Chem. 117 (1997) 449-454.

[62] W. R. Thiele, Chem. Ber. 129 (1996) 575-580.

[63] S. M. Bruno, B. Monteiro, M. S. Balula, C. Lourenço, A. A. Valente, M. Pillinger, P. Ribeiro-Claro, I. S. Gonçalves, Molecules 11 (2006) 298-308.

[64] S. Figueiredo, A. C. Gomes, J. A. Fernandes, F. A. A. Paz, A. D. Lopes, J. P. Lourenço, M. Pillinger, I. S. Gonçalves, J. Organomet. Chem. 723 (2013) 56-64.

[65] M. Bagherzadeh,, H. Mohammadabadi, S. Abednatanzi, A. Abbasi, M. Amini, Nanochem. Res. 2 (2017) 179-187.

[66] L. F. Veiros, A. Prazeres, P. J. Costa, C. C. Romão, F. E. Kühn, M. J. Calhorda, Dalton Trans. (2006) 1383-1389.

[67] C. Dinoi, M. Ciclosi, E. Manoury, L. Maron, L. Perrin, R. Poli, Chem. Eur. J. 16 (2010) 9572-9584.

[68] P. J. Costa, M. J. Calhorda, F. E. Kühn, Organometallics 29 (2010) 303-311.

[69] A. Comas-Vives, A. Lledós, R. Poli, Chem. Eur. J. 16 (2010) 2147-2158.

[70] M. J. Calhorda, P. J. Costa, Curr. Org. Chem. 16 (2012) 65-72.

[71] C. Dinoi, R. Poli, L. Perrin, L. Maron, Dalton Trans. 41 (2012) 1131-1133.

[72] P. Sözen-Aktas, E. Manoury, F. Demirhan, R. Poli, Eur. J. Inorg. Chem. (2013) 2728-2735.

[73] https://www.lyondellbasell.com/globalassets/documents/chemicals-technical-literature/t-hydro-product-safety-bulletin-3453.pdf. Consulted on the 3rd February 2018.

[74] https://www.lyondellbasell.com/en/about-us/company-investments/; https://www.lyondellbasell.com/en/products-technology/chemicals/chemical-type/peroxides/. Consulted on the 3rd February 2018.

[75] http://www.huntsman.com/performance_products/a/Home/Technology%20licensing. Consulted on the 3rd February 2018.

[76] I.V. Kozhevnikov, G.P. Mulder, M.C. Steverink-de Zoete, M.G. Oostwal, J. Mol. Catal. A: Chem. 134 (1998) 223–228.

[77] E. Poli, R. De Sousa, F. Jérome, Y. Pouilloux, J.-M. Clacens, Catal. Sci. Technol. 2 (2012) 910–914.

[78] A. Enferadi-Kerenkan, A. Gandon, T. O. Do, Dalton Trans. 47 (2018) 1214–1222.

Figure Captions

Figure 1. Asymmetric unit, (b) fragment of (1-D) anionic chain, (c) unit cell projection of methylammonium ammonium trimolybdate **1**.

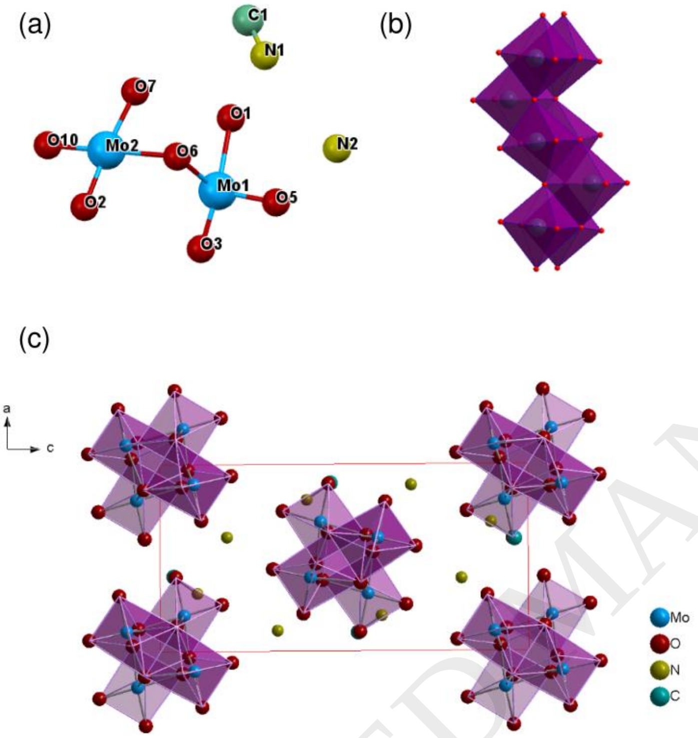

Figure 2 (a) Asymmetric unit, (b) (2-D) anionic layer, (c) unit cell projection of bis(2,5-dimethylanilinium) pentamolybdate **4**.

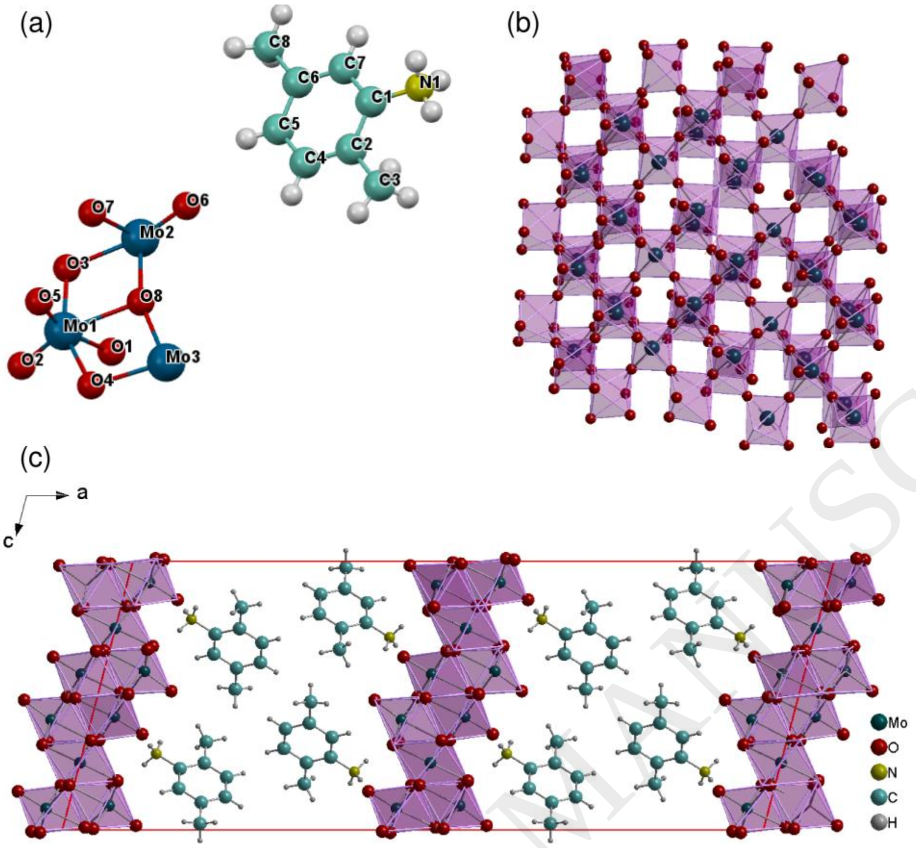

Figure 3. Catalyst stability of **4-7** (6 h runs) or **2** and **3** (1 h runs), using Cy as model substrate, at 70 °C (CyO selectivity was always 100 %).

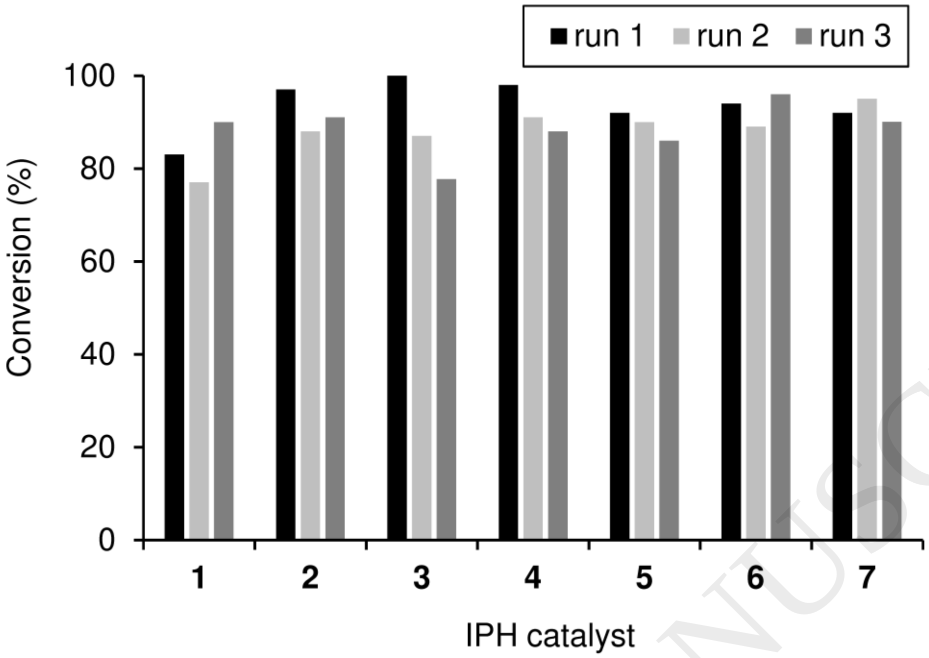

Figure 4. FT-IR spectra (A, C, E) and XRPD patterns (B, D, F) of the original and reused catalysts (three batch runs): **1** (A, B), **2** (C, D) and **4** (E, F).

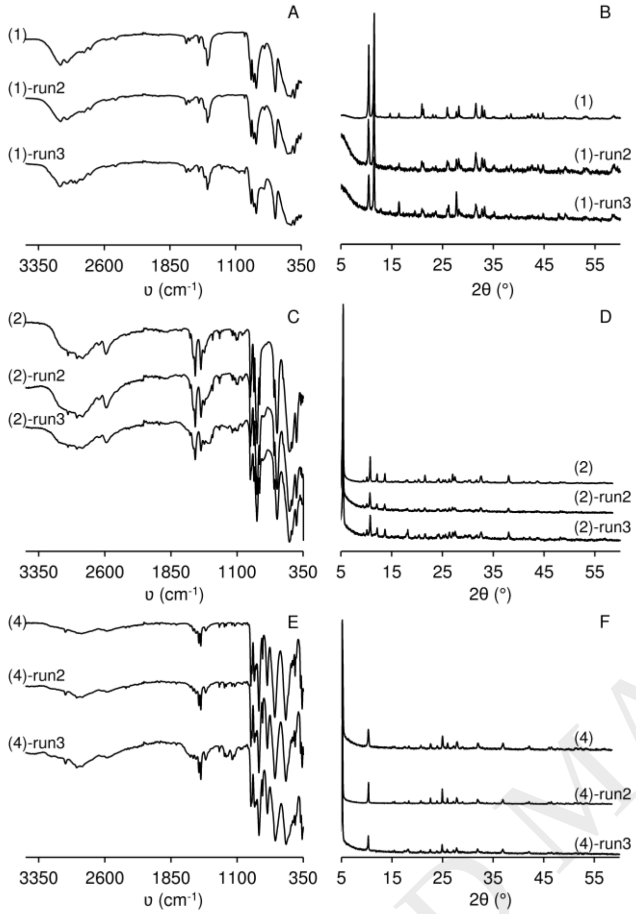

Figure 5. FT-IR spectra (A, C) and XRPD patterns (B, D) of the original and reused catalysts (three batch runs): **5** (A, B), **6** (C, D) and **7** (E, F).

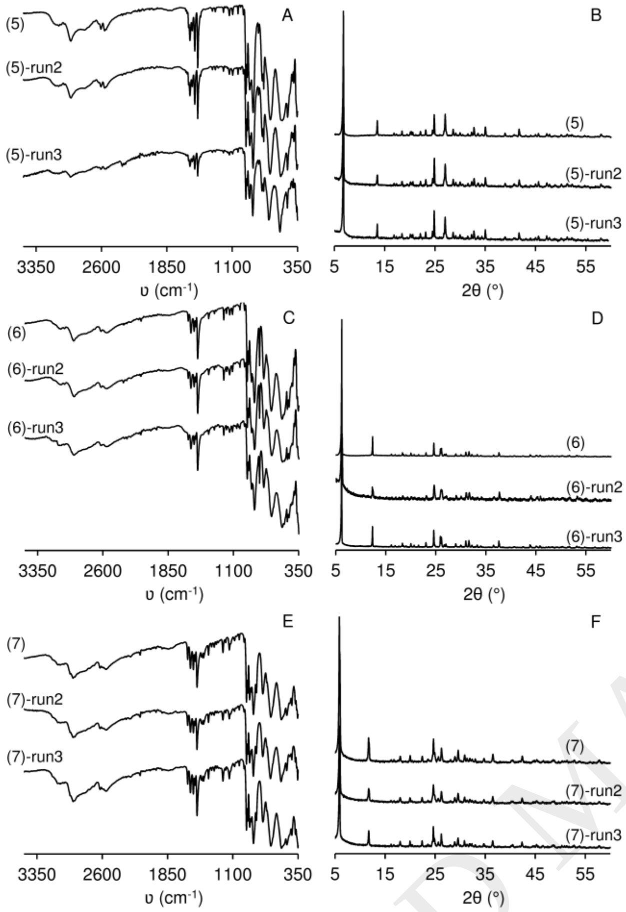

Figure 6. SEM images for (a) **1**, (b) (**1**)-run2, (c) **2**, (d) (**2**)-run2, (e) **4**, (f) (**4**)-run2, (g) **5**, (h) (**5**)-run2, (i) **6**, (j) (**6**)-run2, (k) **7** and (l) (**7**)-run2.

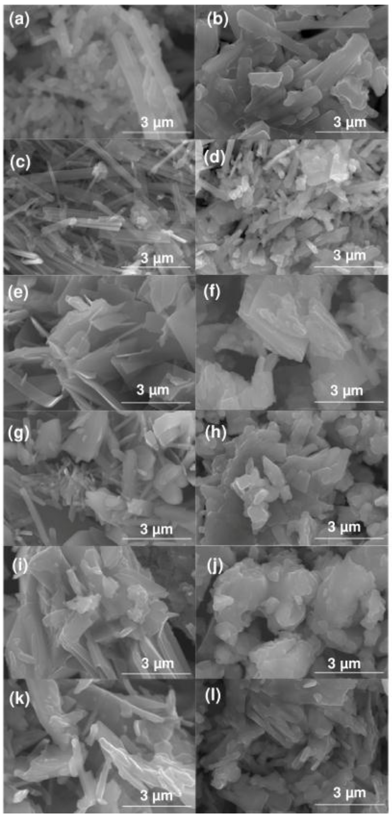

Figure 7. Initial catalytic activity of the anilinium-based IPHs for Cy epoxidation: (a) relation with structure dimensionality; (b) initial activity versus the distance between layers/chains (for compounds **2**-**7**).

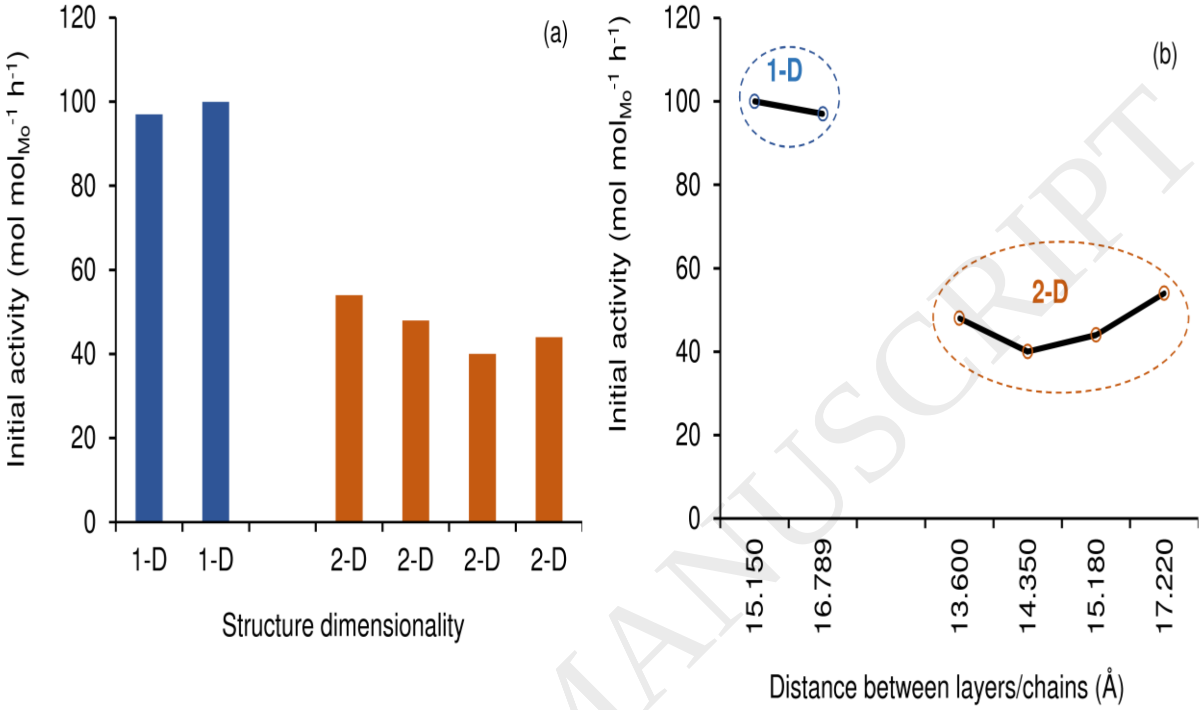

Figure 8. Kinetic profiles of the epoxidation of Ole (□), LinOle (using molar ratio substrate:tbhp = 1.5 (o) or 2.5 (-)), or Lim (×), in the presence of **2**, at 70 °C. Error bars are included. The inset is a more detailed view of the intial kinetics.

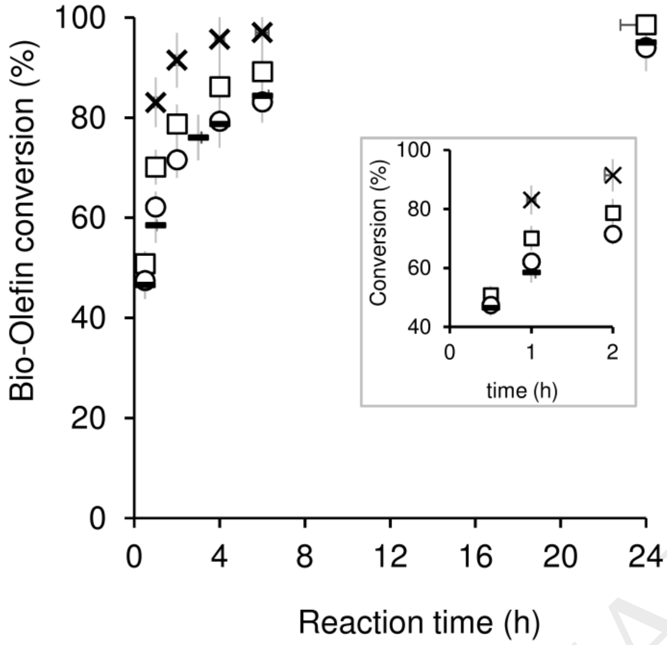

Figure 9. Dependency of bio-product yields on the conversion of the FAMEs (a) Ole or (b) LinOle (LinOle:tbhp = 1.5 (solid lines) or 2.5 (dashed lines), in the presence of **2**, at 70 °C. The bio-products were: (a) OleOx (o); (b) LinOleOx ((Δ) for LinOle:tbhp = 1.5; (×) for LinOle:tbhp = 2.5), LinOleDiox ((□) for LinOle:tbhp = 1.5; (-) for LinOle:tbhp = 2.5), and cyclisation products ((◊) for LinOle:tbhp = 1.5; (+) for LinOle:tbhp = 2.5).

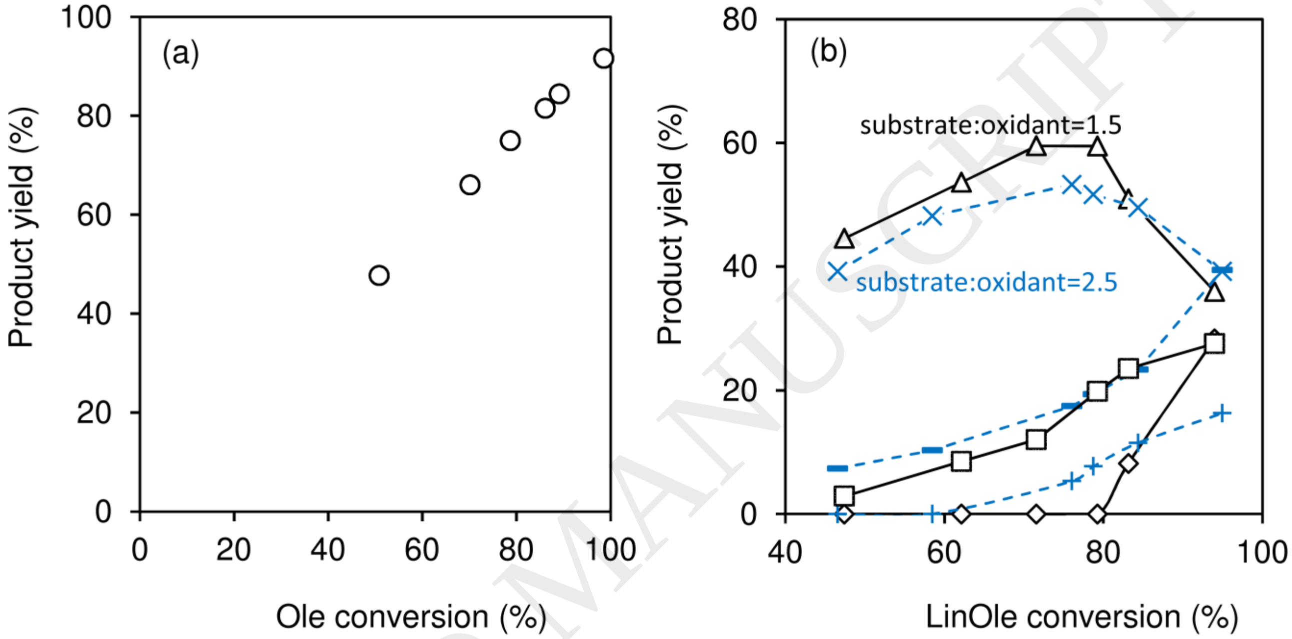

Figure 10. Dependency of LimOx (Δ), LimDiOx (□) and LimDiOH (◊) yields on Lim conversion, in the presence of **2**, at 70 °C.

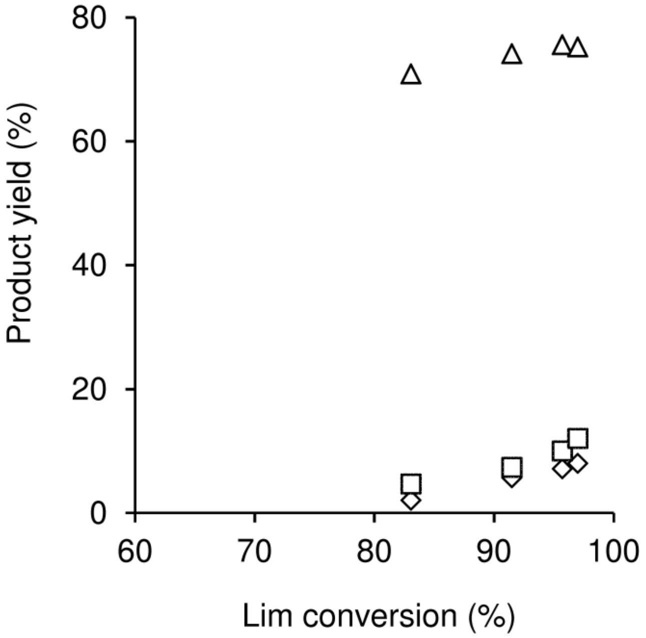

Scheme 1. Biomass-derived olefins converted to useful products, in the presence of molybdenum-based catalysts studied in this work.

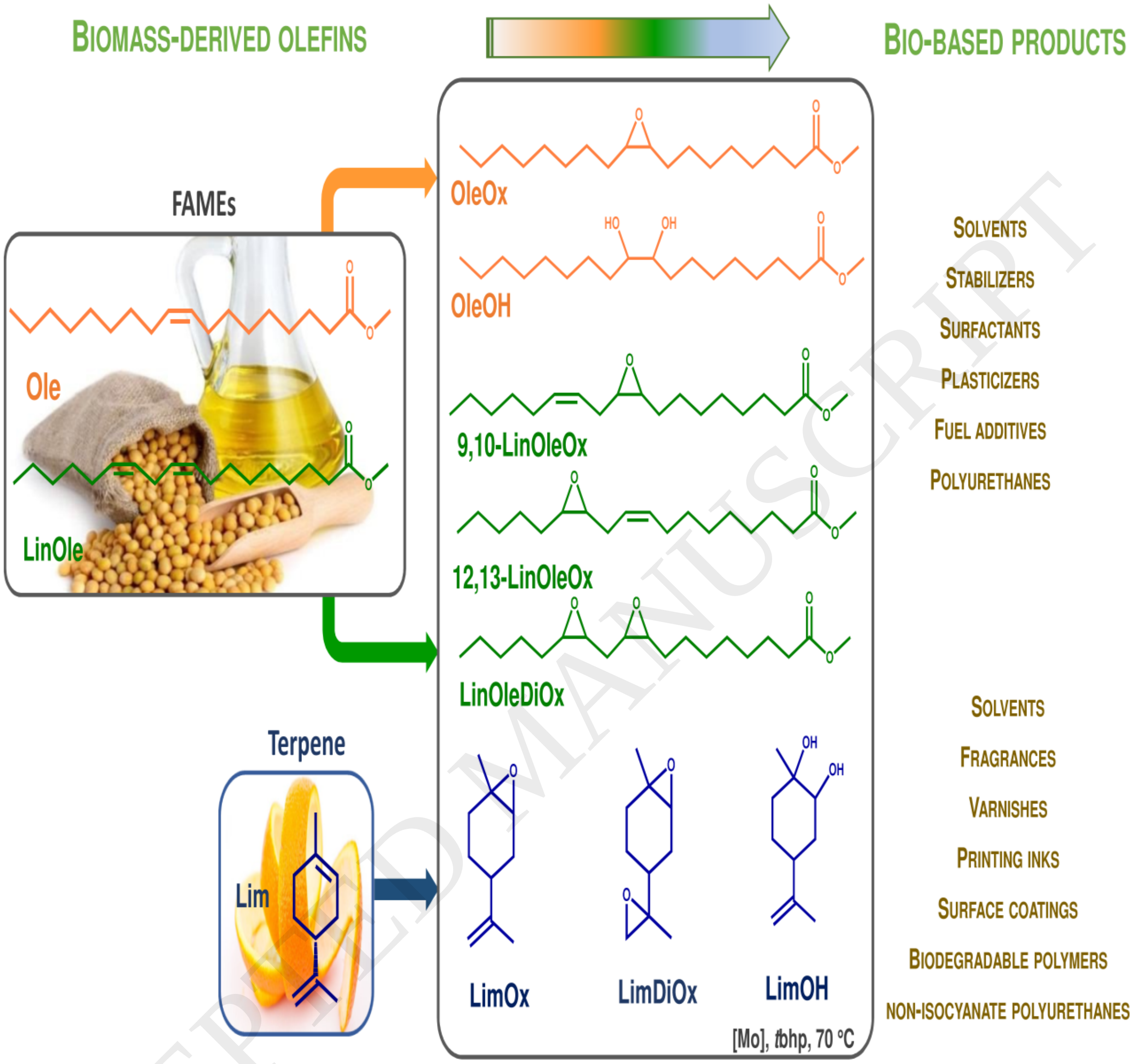

Table 1. Crystal and structure refinement data from XRPD studies of **1** and **4**.

Compound name / code	Methylammonium ammonium trimolybdate **1**	Bis(2,5-dimethylanilinium) pentamolybdate **4**
CCDC code	**CCDC 1586678**	**CCDC 1586679**
Empirical formula	$CH_{10}N_2Mo_3O_{10}$	$C_{16}H_{24}Mo_5N_2O_{16}$
Moiety formula	Mo_3O_{10}, (CH_3NH_3), (NH_4)	Mo_5O_{16}, $2(C_8H_{12}N)$
Formula weight [g/mol]	497.9178	692.19
Temperature [K]	293(2)	293(2)
Wavelength [Å]	1.54060	1.54178
XRPD measurement	X'PERT PRO mpd, Bragg - Brentano geometry	X'PERT PRO mpd, DSH geometry with focusing mirror
Crystal system, space group	orthorhombic P nma	monoclinic, C 2/c
Unit cell dimensions [Å, °]	8.6857(10), 7.620(3), 17.056(2), 90.0, 90.0, 90.0	35.6001(11), 5.53576(18), 14.1830(4), 90.0, 104.653(3), 90.0
Volume [Å^3]	1128.8(4)	2704.19
Z, Calculated density [Mg/m$^{3]}$	4, 2.873	4, 2.407
Absorption coefficient [mm^{-1}]	2.229	19.18
F(000)	936	1888
2Theta range, step size [°]	3.0-75, 0.02	3.0, 90, 0.02
Index ranges (h, k, l = max)	6, 6, 13	32, 5, 13
Refinement method	Restrained Rietveld refinement	restrained Rietveld refinement

Number reflections/data points	325 / 3600	1089 / 4350
Number of atoms/ parameters/restraints	12, 36, 20	32, 86, 35
Goodness-of-fit	8.45	4.33
Final R_{wp}/R_p factors	R_p = 0.0749, R_{wp} = 0.1086	R_p = 0.0542, R_{wp} = 0.0768
R_F and wR_F factor	R_F = 0.0382, wR_F = 0.0532	R_F = 0.0335, wR_F = 0.0464
<shift/su>	0.0078	0.0063

Table 2. Selected bond lengths in compound **1**.

Atoms [symmetry operations]		**Bond length [Å]**
Mo1	O3	1.697(12)
Mo1	O5	1.692(14)
Mo1	O6	1.917(7)
Mo1	O7 [-x, -0.5+y, -z]	1.978(8)
Mo1	O1	2.278(16)
Mo1	O1 [-x, -y, -z]	2.380(15)
Mo2	O2	1.766(18)
Mo2	O10	1.760(18)
Mo2	O1 [-x, 0.5+y, -z]	2.03(2)
Mo2	O1 [-x, -y, -z]	2.03(2)
Mo2	O6	2.38(3)
Mo2	O7	2.23(3)

Table 3. Selected bond lengths in compound **4**.

Atoms [symmetry operations]		**Bond length [Å]**
Mo1	O5	1.70(2)
Mo1	O2	1.72(1)
Mo1	O3	1.96 (2)
Mo1	O4	1.93 (2)
Mo1	O1	2.07 (3)
Mo1	O8 [1-x, y, 0.5-z]	2.34(2)
Mo2	O6	1.68(1)
Mo2	O3 [x, 1-y, -0.5+z]	1.95(3)
Mo2	O1 [x, -y, -0.5+z]	2.01(3)
Mo2	O8	2.02 (2)
Mo2	O7	2.13(2)
Mo2	O3 [1-x, y, 0.5-z]	2.23(2)
Mo3	O8 [x, -y, 0.5+z]	1.98(2)
Mo3	O8 [1-x, -y, 1-z]	1.98(2)
Mo3	O7 [x, 1-y, 0.5+z]	1.99 (2)
Mo3	O7 [1-x, 1-y, 1-z]	1.99 (2)
Mo3	O4 [1-x, -y, 1-z]	2.19(1)
Mo3	O4 [x, -y,0.5+z]	2.19(1)

Table 4. Epoxidation of cis-cyclooctene with tbhp, in the presence **1**-**7**.[a]

Catalyst	Temperature (°C)	CyO yield (%) at 1 h/6 h/24 h	Initial activity [b] (mol mol_{Mo}^{-1} h^{-1})
1	70	24/83/100	24
2	55	71/100/-	71
2	70	97/100/-	97
3	55	91/100/-	91
3	70	100/-/-	100
4	70	54/98/100	54
5	70	48/92/100	48
6	70	40/94/100	40
7	70	44/92/100	44

[a] Reaction conditions: initial molar ratio Mo:Cy:oxidant = 1:100:153, $[Cy]_0$ = 1.0 M; 1 mL tft. [b] Cyclooctene oxide (CyO) yield (CyO selectivity was always 100 %. [b] Initial activity (or turnover frequency) calculated for 1 h reaction.

Table 5. Epoxidation of cis-cyclooctene with tbhp, in the presence **2** or **3**, and comparison to literature data[a]

Catalyst [b]	T (°C)	Solv.	Mo:Cy:Ox	CyO yield (%) at 1/6/24 h	Ref.
2	55	tft	1:100:152	71/100/-	-
2	70	tft	1:100:152	97/100/-	-
3	55	tft	1:100:152	91/100/-	-
3	70	tft	1:100:152	100/-/-	-
MoO_3	70	tft	1:100:152	4/71/96	-
Molybdic acid	70	tft	1:100:152	4/96/100	-
$(H_3biim)_4[\beta\text{-}Mo_8O_{26}]$	55	tft	1:100:152	21/62/93	29
$(H_3biim)_4[\beta\text{-}Mo_8O_{26}]$	70	tft	1:100:152	45/86/97	29
$(Himi)_4[(imi)_2Mo_8O_{26}]\cdot H_2O$	35	$CHCl_3$	1:21:21	-/82/-	23
$(Himi)_4[(imi)_2Mo_8O_{26}]\cdot H_2O$	45	$CHCl_3$	1:21:21	-/89/-	23
$(H_2bbi)_2[Mo_8O_{26}]$	45	$CHCl_3$	1:21:21	-/64/-	23
$(H_2bbi)[(H_2bbi)_2(Mo_8O_{26})]\cdot H_2O$	45	$CHCl_3$	1:21:21	-/60/-	23
$[H(atrz)]_4[(atrz)_2(Mo_8O_{26})]\cdot 2H_2O$	45	$CHCl_3$	1:25:25	-/80/-	45
$(NH_4)_4[Mo_8O_{26}]$	rfl [c]	CH_3Cl	1:25:45	98 (2 h)	46
$(4,4'\text{-}H_2bipy)[Mo_7O_{22}].H_2O$	rfl [c]	CH_3CN	1:24:73	>99 (14 h)	31
$(IMesH)_2[Mo_6O_{19}]$	55	-	1:17:33	~43 (24 h)	47
$[MoO_2(HL^1)]_2[Mo_6O_{19}]$	80	-	1:286:571[d]	72[e] (6 h)	48
$[MoO_2(HL^2)]_2[Mo_6O_{19}]$	80	-	1:286:571 [d]	72[f] (6 h)	48
$[MoO_2(HL^3)]_2[Mo_6O_{19}]$	80	-	1:286:571 [d]	76 [g] (6 h)	48
$(Bu_4N)_2[Mo_6O_{19}]$	80	-	1:667:1333 [d]	30 [f] (6 h)	48
$(Bu_4N)_2[Mo_6O_{19}]$	80	dce	1:167:167 [d]	10 (5 h)	49
$[MoO_2(HL^4)(H_2O)]_2[Mo_6O_{19}]\cdot 2MeCN$	60	dce	1:143:143 [d]	82 (5 h)	49
$(Bu_4N)_2[Mo_6O_{19}]$	55	CH_3CN[i]	1:16:39	13 h[h] (3.5 h)	50
$[(n\text{-}C_4H_9)_4P]_2[Mo_6O_{19}]$	60	CH_3CN	1:17:33	30 (4 h)	51

$[\{MoO_2(HC(3,5\text{-}e_2pz)_3)\}_2(\mu_2\text{-}O)][Mo_6O_{19}]$	55	dce	1:100:152	-/46/87	30
$[Mo(O)_2(salen)$–POM]	75	dce	1:50:150	100 (6 h)	52
$[MoO_2(acac)$–POM]	75	dce	1:63:188	100 (8 h)	53

[a] Reaction conditions: T = temperature, Solv = co-solvent, Mo:Cy:Ox = molar ratio Mo:Cy:tbhp. Cycloctene epoxide yield at 1 h/6 h/24 h reaction (unless otherwise specified in parenthesis); CyO selectivity ≥ 99 % (unless otherwise specified). [b] H_2biim = 2,2'-biimidazole; imi = imidazole, H_2bbi = 1,1'-(1,4-butanediyl)bis(imidazolium); atrz = 3-amino-1,2,4-triazole; 4,4´-bipy = 4,4´-bipyridine; IMes=1,3-bis(2,4,6-trimethylphenyl)imidazol-2-ylidene; H_2L^1=pyridoxal isonicotinic acid hydrazone, H_2L^2 = pyridoxal benzhydrazone; H_2L^3=pyridoxal 4-hydroxy benzhydrazone; Bu_4N=tetrabutylammonium; H_2L^4 = (*E*)-2-((2-(benzo[*d*]thiazol-2-yl)hydrazono)methyl)-6-methoxyphenol; $HC(3,5\text{-}Me_2pz)_3$ = tris(3,5-dimethyl-1-pyrazolyl)methane; acac=acetylacetonate; the Keggin-type POM unit is related to the anion $[SiW_{11}O_{39}]^{8-}$. [c] rfl = reflux. [d] 70 % aqueous *t*bhp was used. [e] CyO selectivity = 58 %. [f] CyO selectivity = 53 %. [g] CyO selectivity = 55 %. [h] CyO selectivity = 13 %. [i] Toluene was also added as co-colvent.

Table 6. Influence of the reaction conditions on the epoxidation of methyl oleate (Ole) with *t*bhp, in the presence **2**.

T (°C)	Cosolvent.	Ole conversion (%) at 1/6/24 h	Methyl 9,10-epoxyoctadecanoate yield (%) at 1/6/24 h
55	tft	2162/80	19/55/74
70	tft	70/89/99	66/84/92
	dce	71/89/95	62/79/87
	tol	63/84/94	58/79/89
	acn	31/70/89	31/69/88
85	tft	90/96/-	81/89/-